

Supporting Information

Liquid Cu-Zn Catalyzed Growth of Graphene Single-crystals

Lin Li,^{1,} Minghui Li,² Ruijie Zhang,² Qing Zhang,² Hang Li,³ Dechao Geng^{2,*}*

¹ College of Chemistry, Tianjin Normal University, Tianjin 300387, P. R. China

² Tianjin Key Laboratory of Molecular Optoelectronic Sciences, Department of Chemistry, School of Science, Tianjin University and Collaborative Innovation Center of Chemical Science and Engineering, Tianjin 300072, P. R. China

Email: linli2023@tjnu.edu.cn, gengdechao_1987@tju.edu.cn

Keywords: Large-scale graphene, Liquid Cu–Zn alloy, Chemical vapor deposition,

Methods

Synthesis of graphene on pure Cu and Cu-Zn alloy: 25 μm thick Cu foils (99.999% purity) and 50 μm thick W foils (99.95%) were obtained from Alfa Aesar. 2-4 pieces of Cu foils were directly placed on W foils for CVD growth of graphene. Prior to graphene growth, the CVD 1 inch quartz tube was pumped to ~ 5 Pa to clean the system, and then filled with 200 standard cubic centimeters per minute (sccm) H_2 followed by heating the furnace to the desired temperature above the melting point of Cu over 30-40 min. Subsequently, annealing for 30 min was employed. At the beginning of growth, the H_2 flow rate was changed to the desired value, and CH_4 was then introduced to the chamber with the required value for a certain time. Finally, CH_4 was turned off, and the system was cooled down to room temperature at the cooling rate of about 25 $^\circ\text{C}/\text{min}$. The growth method of Cu-Zn alloy is similar to the above, in which the proportion of alloy is changed by weighing the weight of Cu and Zn foil.

Characterization Methods: SEM measurements were conducted on the FEI Verios 460 field emission scanning electron microscope. Out-of-plane XRD patterns were recorded by Rigaku SmartLab X-ray diffraction with a power of 9 kW, a monochromatic radiation of Cu $\text{K}\alpha$ ($\lambda = 1.5406 \text{ \AA}$), and a BB measurement mode. TEM, HRTEM, and SAED measurements were conducted on JEM-2800. Raman mapping was tested on the Horiba Labram HR Evolution. XPS spectra were collected on an ESCALAB-250Xi spectrometer using monochromatic Al- $\text{K}\alpha$ ($h\nu = 1486.6 \text{ eV}$) radiation.

Electrical characterization of large-scale graphene uniformity: The electrical properties of HGFs and their continuous films were measured after they were transferred onto 300 nm SiO_2/Si substrates. FET devices based on HGFs were fabricated using our previous method. Briefly, 2-5 μm wide nanowires (a rigid "H" type anthracene derivative) were deposited on individual HGFs, and then a 30 nm gold film was evaporated on the sample. Finally, the nanowires were removed by a micromanipulator, and the desired electrodes were fabricated by mechanically scratching the gold film in order to make isolated FET devices. In the case of the graphene film device, Au electrodes were directly deposited through shadow masks, and then shaped to short widths by manipulator scratching. The tests, including measuring I-V curves and back-gated FET

properties of HGFs and films, were conducted with a Keithley 4200 analyzer at room temperature in air, and 2-D resistivity and saturation current density for graphene\ and films were calculated from the data.

The mobility of charge carriers is extracted from the equation:
$$\mu_{dev} = \frac{L}{V_D C_{ox} W} \cdot \frac{dI_d}{dV_g}$$
, where L and W are the device channel length and width, V_D is the voltage between source and drain electrodes, and C_{ox} is the gate capacitance per unit area.

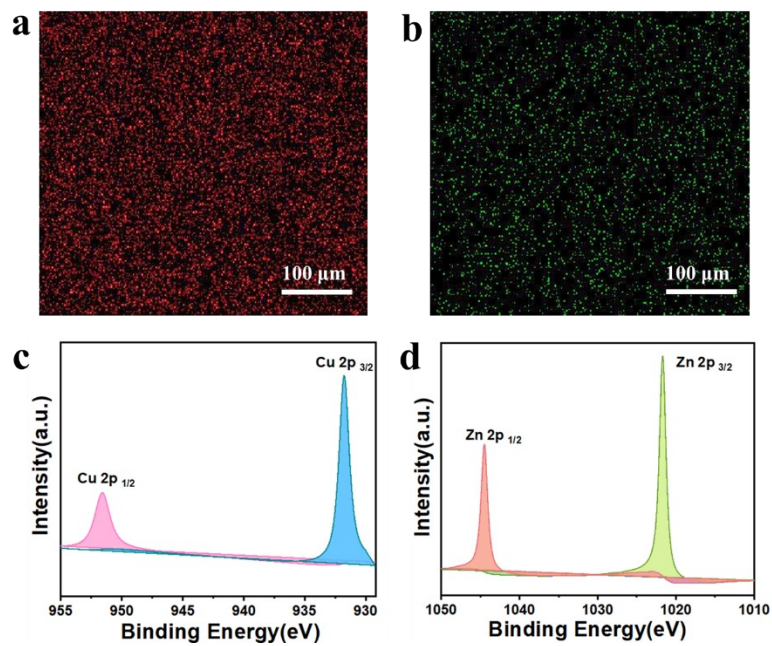


Figure S1. Characterization of Cu-Zn alloy substrate, (a-b) EDX mapping of metallic Cu (red) and Zn (green), (c-d) XPS spectra of Cu and Zn.

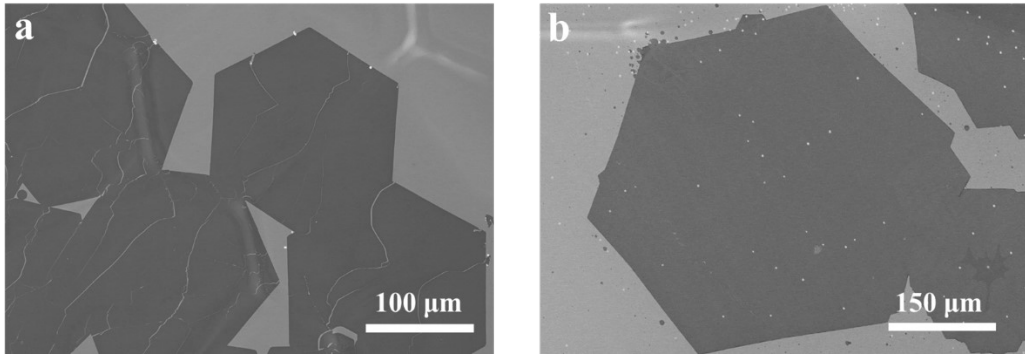


Figure S2. SEM images of graphene on the surface of liquid pure Cu (a) and Cu-Zn alloy (b).

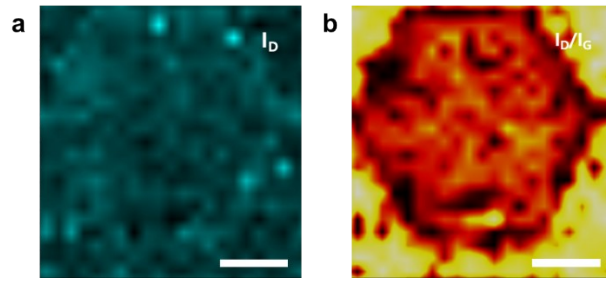


Figure S3. Raman mapping results of the large-area graphene. (a) D peak mapping result, in which the signal of defect is weak. (b) Raman mapping of I_D/I_G . The scale bars are 0.1 mm.

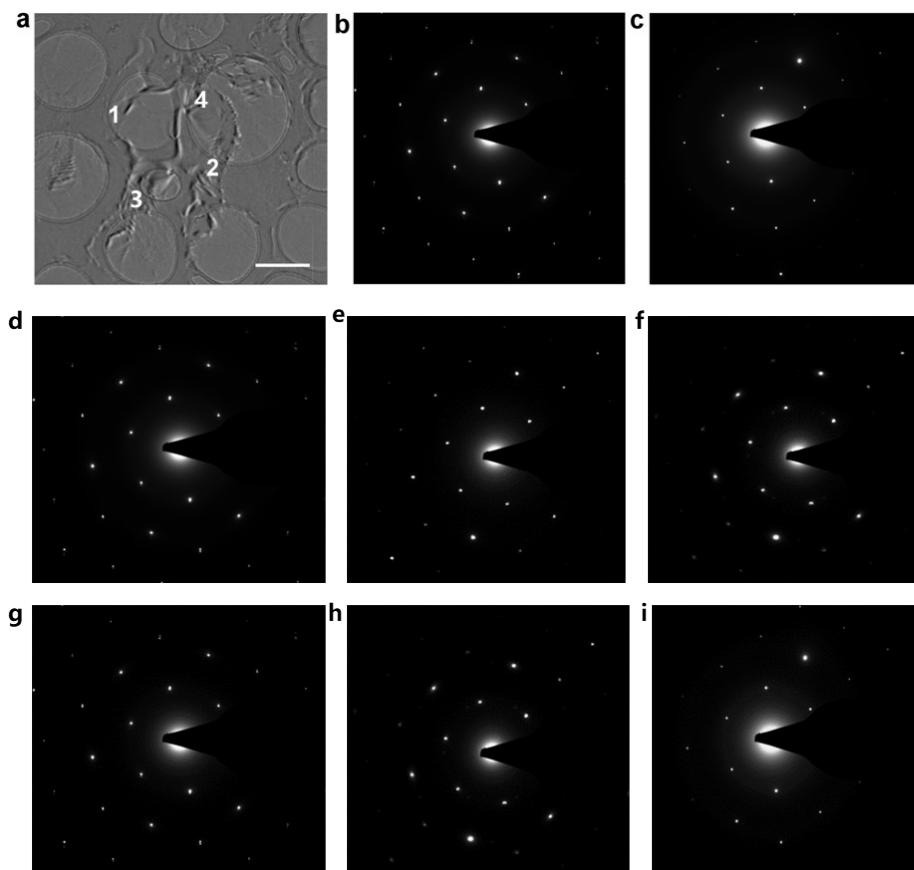


Figure S4. (a) TEM image together with SEAD patterns on different locations of whole graphene surface showing the same set of six-fold symmetric diffraction points, indicating the single-crystalline nature of graphene. (b-i) Eight representative SAED patterns taken from different grid holes as indicated in (a)

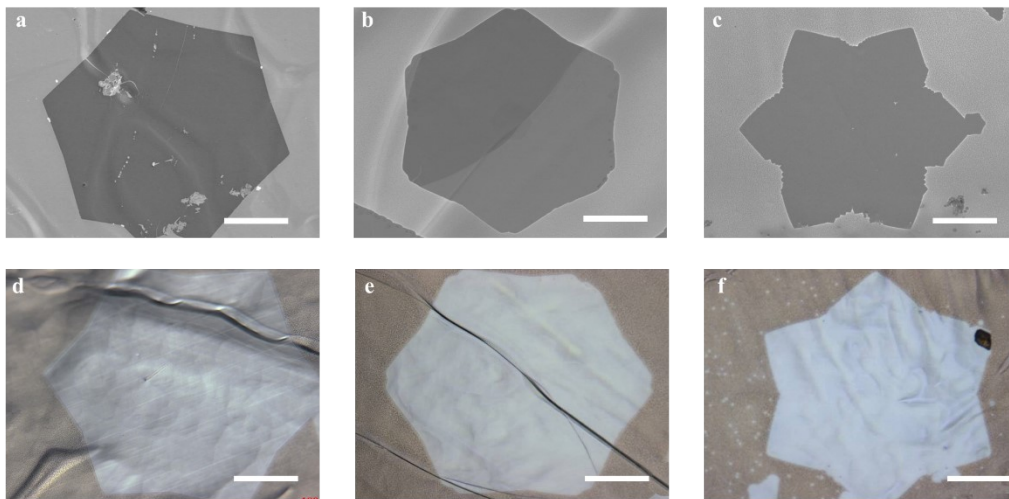


Figure S5. Optical and SEM images of graphene with different boundaries, the scale bars are 100 μm .

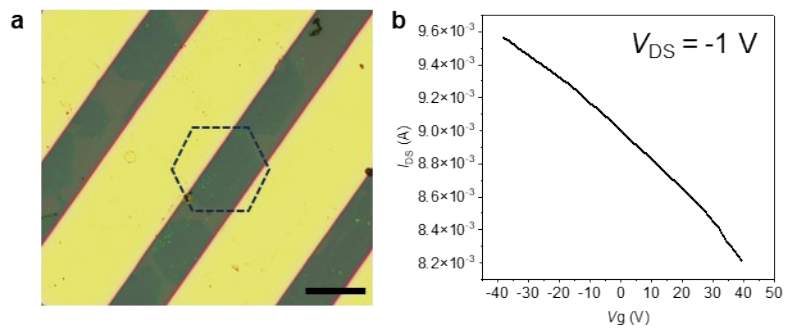


Figure S6. The FET based on as-produced graphene. (a) Optical image of the FET. The scale bar is 20 μm .

(b) Typical transfer curve.

Table S1. Growth conditons of graphene samples.

| Figure | Temperature (°C) | CH ₄ (sccm) | Ar (sccm) | H ₂ (sccm) | Time (min) |
|--------|------------------|------------------------|-----------|-----------------------|------------|
| S4a、 d | 1090 | 0.5 | 500 | 3 | 6 |
| S4b、 e | 1090 | 0.5 | 550 | 3 | 6 |
| S4c、 f | 1090 | 0.5 | 580 | 3 | 6 |

Supporting Note S1

With the increase of Zn content in a certain range, we observed the decreased nucleation density, but the increased grain size of graphene. Moreover, the edge of hexagonal graphene crystal is almost parallel to a line, indicating that the grown graphene array has excellent orientation uniformity. This may be attributed to the same electrostatic repulsion in each direction of graphene single crystal. According to the literatures, the catalytic decomposition of methane and the solubility of carbon of metal Zn are far lower than that of Cu. Cu-Zn alloy forms an ideal smooth and uniform liquid surface when heated to the melting point. Zn atoms effectively reduce the density of Cu atoms on the alloy liquid surface, for which the increase of Zn element will inhibit the nucleation ability of graphene on the alloy substrate. Therefore, we provided a low-cost and controllable strategy for preparing large-size graphene arrays. The size of graphene was controlled by the proportion of alloy introduced, and the range is from tens of microns to hundreds of microns.

Supporting Note S2

First, after dehydrogenation of the carbon source, activated carbon atoms are formed on the surface of Cu and in the gas phase. Compared with gas-phase reaction, dehydrogenation of carbon source on metal substrate is more favorable. At the same time, there is a dynamic balance between the adsorption and desorption of carbon source on the Cu surface. Then the activated carbon diffuses to the Cu surface, aggregates at the active sites on the Cu substrate to form graphene nucleation seeds, and then diffuses to the edge of graphene core to expand the size of graphene domain. It should be noted that controlling the nucleation density in the nucleation step is very important for the synthesis of large area single crystal graphene.

Supporting Note S3

In Cu-Zn alloy with low Zn content, it is mainly affected by the nucleation and growth of Cu surface. The introduction of Zn on the surface of liquid Cu will first inhibit the adsorption and decomposition of methane on the alloy substrate and reduce the number of activated carbon sources on the surface of the growth substrate. In principle, size of graphene is determined by the competition between graphene nucleation and grain growth processes. Lower nucleation density and higher growth rate result in graphene flakes with average large size. In the case of reasonable growth rate, the graphene size is a direct reflection of nucleation densities. In the classical theory of nucleation, nucleation process is a critical step associated with a critical nucleus size formulated by Gibbs-Thomson equation that is due to competition between energy gain and creation of new surface free energy involved in phase transformation process. The ease of nucleation is thus related to the surface free energy that will be replaced with surface of new nucleation phase. This rule usually leads to a significant barrier for homogeneous nucleation occurring that is related to a critical supersaturation condition to initiate. In contrast, heterogeneous nucleation, *i.e.*, nucleation occurred on foreign substrates easily occurs at a lower supersaturation condition. In the case of graphene growth on solid Cu surface, the nucleation preferentially occurs on grain boundaries, steps or defects associated with higher surface energy, resulting in a non-uniform graphene. We introduced Zn atom to the surface of Cu to form a solid solution, which would lengthen the lattice structure of Cu, and the energy trough would appear on the crystal surface of the alloy suitable for graphene growth, and finally formed a lower number of nucleation sites on the surface of the alloy than on the surface of pure Cu. Under this circumstance, the Cu-Zn alloy substrate owned the effect of inhibiting the nucleation density of graphene, while grown into a large-size single-crystal graphene crystal domain under the continuous supply of low active carbon source